



Cite this: *Chem. Commun.*, 2025, 61, 16954

Received 7th August 2025,
 Accepted 29th September 2025

DOI: 10.1039/d5cc04527d

rsc.li/chemcomm

Photo-induced ruthenium-catalyzed alkene C–H-arylation at room temperature

Tanumoy Mandal,^a Stéphane Golling,^a Sven Trienes^{ib,ab} and Lutz Ackermann^{ib,*ab}

C–H arylation has surfaced as a powerful tool for molecular sciences, with alkene C–H arylation thus far requiring either high reaction temperatures of 120 °C or stoichiometric amounts of RMgX. In sharp contrast, we herein report on room-temperature C–H arylations of alkenes by means of ruthenium(II) catalysis with ample scope. This strategy also enabled late-stage diversification of structurally complex molecules and mechanistic studies provided strong evidence for photo-excitation of a ruthenacycle intermediate.

Transition metal catalysis has emerged as a transformative platform for the interconversion of functional groups, enabling the assembly of valuable organic molecules. Particularly, C–H activation represents arguably the most efficient strategy, avoiding lengthy and resource-demanding multi-step syntheses.¹ The introduction of an aryl motif *via* C–H arylation provided access to distinct molecules by means of ruthenium catalysis,² with various applications to crop protection, polymer chemistry, and drug discovery, among others.^{3,4} While most C(sp²)–H functionalizations predominantly focus on arene C–H bonds, the direct activation of vinylic C–H bonds continues to be underdeveloped.⁵ Thus, previous alkene C–H arylations relied as of yet on either high reaction temperatures of 120 °C,^{6–10} or very reactive Grignard reagents in stoichiometric amounts,¹¹ thus severely compromising the viable functional group tolerance (Scheme 1A). In sharp contrast, we herein report on the unprecedented C–H-arylation of alkenes at ambient temperature. Key to success was represented by the unique features of light-enabled^{12–16} ruthena(II)¹⁷ photoredox catalysis, enabling efficient arylations of alkenes and 1,3-dienes with outstanding levels of chemo-, diastereo- and site-selectivities (Scheme 1B). Late-stage diversifications proved thereby viable at ambient temperature, while detailed mechanistic studies were

suggestive of the photo-MLCT-excitation of the key ruthenacycle intermediate.

At the outset of our studies, vinylpyridine **1a** and 4-iodoanisole **2a** were probed for the photo-induced C(sp²)–H-arylation. Gratifyingly, with Na₂CO₃ as the base, 10 mol% of [Ru(OAc)₂(*p*-cymene)] as the catalyst in a mixture of DMA/1,4-dioxane (3 : 1), the corresponding tri-substituted olefin **3a** was obtained in 81% yield (Table 1, entry 1). Lower catalytic performances were observed in 1,4-dioxane, DMA, or other solvent mixtures such as DMA/THF in a 3 : 1 ratio (entries 2 and 3). An inferior catalytic efficacy was observed with K₂CO₃ or K₃PO₄ as the base (entry 4). [Ru(MesCO₂)₂(*p*-cymene)] as the catalyst furnished the corresponding product **3a** in a satisfying yield of 72% (entry 5). Interestingly, the use of the dimeric [RuCl₂(*p*-cymene)]₂ resulted in a lower yield of 32% which can be improved to 79% by adding a catalytic amount of NaOAc (entry 6), highlighting the importance of carboxylate assistance for efficient C–H activation.¹⁸ However, additional studies indicated a broader applicability and efficacy with [Ru(OAc)₂(*p*-cymene)] as compared to [RuCl₂(*p*-cymene)]₂ in combination with acetate additives (see SI for



Scheme 1 (A) Previous work on directed, transition-metal-catalyzed arylation of alkenes. (B) This work: photo-induced ruthenium-catalyzed C–H-arylation of alkenes.

^a Wöhler Research Institute for Sustainable Chemistry (WISCh), Georg-August-Universität Göttingen, Tammannstraße 2, 37077 Göttingen, Germany. E-mail: Lutz.Ackermann@chemie.uni-goettingen.de

^b DZHK (German Centre for Cardiovascular Research), Potsdamer Straße 58, 10875 Berlin, Germany



Table 1 Optimization studies^a


| Entry | Deviation from standard conditions | Yield 3a ^b (%) |
|----------------|---|--------------------------------|
| 1 | None | 81 |
| 2 | 1,4-Dioxane or DMA as sole solvent | 31/48 |
| 3 ^c | DMA/THF (3:1) as solvent | 72 |
| 4 | K ₂ CO ₃ or K ₃ PO ₄ as base | 74/65 |
| 5 | [Ru(MesCO ₂) ₂ (<i>p</i> -cymene)] as catalyst | 72 |
| 6 | [RuCl ₂ (<i>p</i> -cymene)] ₂ as catalyst | (32), 79 ^d |
| 7 | RuCl ₃ ·10H ₂ O or Ru ₃ (CO) ₁₂ as catalyst | 0 ^d /0 ^d |
| 8 | Ar–Br, Ar–Cl, or Ar–OTf as arylating reagent | 44/27/(19) |
| 9 | No light | (9) |
| 10 | Without Na ₂ CO ₃ | (12) |
| 11 | Under air | 0 |
| 12 | Without [Ru(OAc) ₂ (<i>p</i> -cymene)] | 0 |

^a Reaction conditions: **1a** (0.5 mmol), **2a** (0.75 mmol), [Ru(OAc)₂(*p*-cymene)] (10 mol%), Na₂CO₃ (2.0 equiv.), N₂, 30 °C, 24 h, DMA/1,4-dioxane (3:1, 1.5 mL), 450 nm blue LED, 30 °C (fan cooling).

^b Isolated yield. Yield in parentheses was determined by ¹H-NMR using CH₂Br₂ as the internal standard. ^c K₂CO₃ (2.0 equiv.) as base.

^d 30 mol% NaOAc as additive.

detailed optimization). Other ruthenium sources, such as Ru₃(CO)₁₂ and RuCl₃·*n*H₂O completely failed to give the desired product **3a** (Table 1, entry 7). Alternative electrophilic aryl donors proved viable, albeit with reduced yields of the desired product **3a** (entry 8). Control experiments reflected the crucial importance of the base and light

irradiation (entries 9–11). The essential role of the ruthenium catalyst was also confirmed (entry 12).

With the optimized reaction conditions for the alkene C–H arylation at room temperature in hand, a viable substrate scope for the photo-induced alkene functionalization was investigated with different aryl iodides. The room-temperature direct arylation proved to be compatible with a large variety of functional groups on electron-rich as well as electron-deficient arenes, including ether (**3a**), ester (**3f**, **3h**), ketone (**3i**), and cyano (**3j**). Halo derivatives were also well tolerated, furnishing the desired products **3l–3n**, featuring valuable electrophilic handles. The synthesis potential of our photo-alkene arylation at room temperature was reflected by the efficient late-stage diversification of (–)-menthol (**3w**), (–)-myrtenol (**3x**), naproxen (**3y**), and indomethacin (**3z**) derivatives (Scheme 2A).

Next, we explored the robustness of the photo-ruthenium-catalyzed C–H arylation at room temperature with a set of representative alkenes **1**. Again, a variety of sensitive functional groups, such as cyano- and halo-substituted substrates, were well tolerated. Notably, a diene furnished product **3aj** with excellent levels of chemo- and site-selectivities. It is noteworthy that a thiazole also enabled chelation-assisted C–H activation, thereby delivering product **3al** in an efficient manner. Additionally, pyrazole was also identified as viable orienting group, furnishing the desired product **3am** (Scheme 2B).

To gain insights into the catalyst's mode of action, we first probed the performance of independently synthesized cyclo-metallated complex **Ru-I**. Interestingly, under photoexcitation, the desired product **3a** was obtained in 77% yield, indicating



Scheme 2 Robustness of the photo-induced C–H activation at room temperature of (A) different aryl iodides and (B) vinyl-heteroarenes. Reaction conditions: **1** (0.5 mmol), aryl iodide **2** (0.75 mmol), [Ru(OAc)₂(*p*-cymene)] (10 mol%), DMA/1,4-dioxane (1.5 mL), 30 °C (fan cooling). The product was obtained as single isomer. If the product was obtained as a mixture of (*Z*) and (*E*) isomers, the ratio is given in parenthesis. More details can be found in the SI. ^a Performed on 0.25 mmol scale.

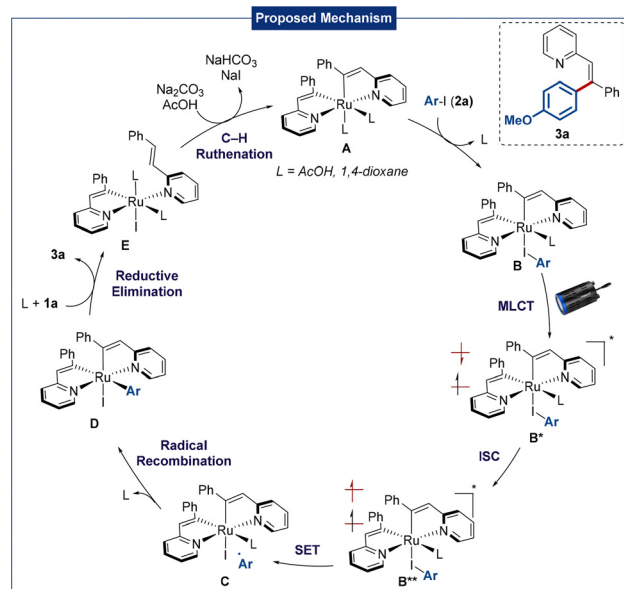




Scheme 3 Key mechanistic findings including (A) reactions with a ruthenacycle, (B) radical scavenger experiments, and (C) on/off experiment.

that a cyclometallated intermediate is likely involved. In contrast, a significantly diminished efficacy was observed in the absence of light at ambient temperature or at 30 °C, highlighting the crucial role of light beyond catalyst activation through *p*-cymene decoordination, being suggestive of photoexcitation of a cyclometallated ruthenium species (Scheme 3A). Second, radical scavenger experiments were performed. While BHT and TEMPO led to strongly diminished yields, galvinoxyl and DPPH completely inhibited the reaction, and the corresponding radical adducts were observed by HRMS, supporting the formation of an aryl radical (Scheme 3B). Third, we analyzed the role of the blue LED irradiation by an on/off experiment, showing a significant inhibition of the reaction in the dark. These findings again suggest that continuous light irradiation is required, hence rendering a sole arene decoordination unlikely to be operative (Scheme 3C). Instead, photoexcitation of a ruthenacycle is more likely. Moreover, a quantum yield of 2% renders a radical chain mechanism unlikely to be operative (see SI for details). Additionally, detailed UV/Vis spectroscopy studies (see SI, Fig. S2) support the formation of a new ruthenium species upon light irradiation. Thus, the generation of a cyclometallated intermediate, most likely, plays a key role in the catalytic cycle.

Based on these mechanistic studies and literature precedents,¹⁷ a plausible mechanism is proposed in Scheme 4. A carboxylate-assisted C–H activation first forms complex **A**, followed by coordination of the aryl iodide to give intermediate **B**,^{17c} which is excited by light to form singlet species **B*** via



Scheme 4 Mechanistic proposal for the ruthenium-catalyzed photoinduced C–H arylation.

MLCT. Intersystem crossing (ISC) then generates the triplet state **B****, enabling SET to generate an aryl radical and complex **C**. Radical recombination results in complex **D**, followed by reductive elimination to afford the desired product **3a** and complex **E** after ligand exchange. Afterwards, further C–H activation leads to the regeneration of the active species **A**.

In conclusion, we reported on a photo-induced C–H arylation of alkenes. Contrary to previous state of the art, the ruthenium catalysis bypasses high temperature or the use of Grignard reagents through photoexcitation and is thereby compatible with a large variety of otherwise sensitive functional groups. Thereby, 39 multi-substituted heterocycle-incorporated olefins were assembled, including several biorelevant derivatives. Mechanistic studies highlighted the crucial role of blue light in this transformation.

The authors gratefully acknowledge generous support by the DZHK, the DFG (Gottfried Wilhelm Leibniz award to L. A.), the ERC Advanced Grant no. 101021358 (L. A.), and DAAD (NAMASTE+) for the financial support (T. M.).

Conflicts of interest

There are no conflicts to declare.

Data availability

All data associated with this study are available in the article and supplementary information (SI). Supplementary information is available. See DOI: <https://doi.org/10.1039/d5cc04527d>.

Notes and references

- (a) T. Rogge, N. Kaplaneris, N. Chatani, J. Kim, S. Chang, B. Punji, L. L. Schafer, D. G. Musaev, J. Wencel-Delord, C. A. Roberts,



- R. Sarpong, Z. E. Wilson, M. A. Brimble, M. J. Johansson and L. Ackermann, *Nat. Rev. Methods Primers*, 2021, **1**, 43; (b) S. Rej, Y. Ano and N. Chatani, *Chem. Rev.*, 2020, **120**, 1788–1887.
- 2 (a) H. Simon, A. Zangarelli, T. Bauch and L. Ackermann, *Angew. Chem., Int. Ed.*, 2024, **63**, e202402060; (b) G. McArthur, J. H. Docherty, M. D. Hareram, M. Simonetti, I. J. Vitorica-Yrezabal, J. J. Douglas and I. Larrosa, *Nat. Chem.*, 2024, **16**, 1141–1150; (c) T. Rogge and L. Ackermann, *Angew. Chem., Int. Ed.*, 2019, **58**, 15640–15645.
- 3 (a) T. Michiyuki, I. Maksso and L. Ackermann, *Angew. Chem., Int. Ed.*, 2024, **63**, e202400845; (b) L. Ackermann, *Org. Proc. Res. Dev.*, 2015, **19**, 260–269; (c) D. A. Horton, G. T. Bourne and M. L. Smythe, *Chem. Rev.*, 2003, **103**, 893–930; (d) J. Hassan, M. Sévignon, C. Gozzi, E. Schulz and M. Lemaire, *Chem. Rev.*, 2002, **102**, 1359–1470.
- 4 (a) S. G. Ouellet, A. Roy, C. Molinaro, R. Angelaud, J.-F. Marcoux, P. D. O'Shea and I. W. Davies, *J. Org. Chem.*, 2011, **76**, 1436–1439; (b) A. Schischko, H. Ren, N. Kaplaneris and L. Ackermann, *Angew. Chem., Int. Ed.*, 2017, **56**, 1576–1580.
- 5 (a) M. Z. Lu, J. Goh, M. Maraswami, Z. Jia, J.-S. Tian and T.-P. Loh, *Chem. Rev.*, 2022, **122**, 17479–17646; (b) J. Zhang, X. Lu, C. Shen, L. Xu, L. Ding and G. Zhong, *Chem. Soc. Rev.*, 2021, **50**, 3263–3314; (c) S. Tang, K. Liu, C. Liu and A. Lei, *Chem. Rev.*, 2015, **44**, 1070–1082.
- 6 S. Oi, K. Sakai and Y. Inoue, *Org. Lett.*, 2005, **7**(18), 4009–4011.
- 7 L. Ackermann, R. Born and P. Ivarez-Bercedo, *Angew. Chem., Int. Ed.*, 2007, **46**, 6364–6367.
- 8 L. Ackermann, R. Vicente, H. K. Potukuchi and V. Pirovano, *Org. Lett.*, 2010, **12**, 5032–5035.
- 9 D. Zell, S. Warratz, D. Gelman, S. J. Garden and L. Ackermann, *Chem. – Eur. J.*, 2016, **22**, 1248–1252.
- 10 M. Kim, J. Kwak and S. Chang, *Angew. Chem., Int. Ed.*, 2009, **48**, 8935–8939.
- 11 L. Ilies, S. Asako and E. Nakamura, *J. Am. Chem. Soc.*, 2011, **133**(20), 7672–7675.
- 12 For representative reviews, see: (a) P. Bellotti, H.-M. Huang, T. Faber and F. Glorius, *Chem. Rev.*, 2023, **123**, 4237–4352; (b) J. Großkopf, T. Kratz, T. Rigotti and T. Bach, *Chem. Rev.*, 2022, **122**, 1626–1653; (c) C.-S. Wang, P. H. Dixneuf and J.-F. Soule, *Chem. Rev.*, 2018, **118**, 7532–7585.
- 13 K. P. S. Cheung, S. Sarkar and V. Gevorgyan, *Chem. Rev.*, 2022, **122**, 1543–1625.
- 14 For rhodium catalysis, see: (a) J. Tanaka, Y. Nagashima, A. J. Araujo Dias and K. Tanaka, *J. Am. Chem. Soc.*, 2021, **143**, 11325–11331; (b) J. Thongpaen, R. Manguin, V. Dorcet, T. Vives, C. Duhayon, M. Mauduit and O. Baslé, *Angew. Chem., Int. Ed.*, 2019, **58**, 15244–15248.
- 15 For copper catalysis, see: (a) S. Trienes, J. Xu and L. Ackermann, *Chem. Sci.*, 2024, **15**, 7293–7299; (b) C. Li, B. Chen, X. Ma, X. Mo and G. Zhang, *Angew. Chem., Int. Ed.*, 2021, **60**, 2130–2134; (c) F. Yang, J. Koeller and L. Ackermann, *Angew. Chem., Int. Ed.*, 2016, **55**, 4759–4762.
- 16 For iron catalysis, see: A. M. Messinis, T. von Münchow, M. Surke and L. Ackermann, *Nat. Catal.*, 2024, **7**, 273–284.
- 17 For recent ruthenium catalysis, see: (a) Y. Wang, S. Chen, X. Chen, A. Zangarelli and L. Ackermann, *Angew. Chem., Int. Ed.*, 2022, **61**, e202205562; (b) J. Struwe, K. Korvorapun, A. Zangarelli and L. Ackermann, *Chem. Eur. J.*, 2021, **27**, 16237–16241; (c) K. Korvorapun, J. Struwe, R. Kuniyil, A. Zangarelli, A. Casnati, M. Waeterschoot and L. Ackermann, *Angew. Chem., Int. Ed.*, 2020, **59**, 18103–18109; (d) A. Sagadevan, A. Charitou, F. Wang, M. Ivanova, M. Vuagnat and M. F. Greaney, *Chem. Sci.*, 2020, **11**, 4439–4443; (e) P. Gandeepan, J. Koeller, K. Korvorapun, J. Mohr and L. Ackermann, *Angew. Chem., Int. Ed.*, 2019, **58**, 9820–9825; (f) T. Michiyuki, I. Maksso and L. Ackermann, *Angew. Chem., Int. Ed.*, 2024, **63**, e202400845; (g) S. Trienes, S. Golling, M. H. Gieuw, M. Di Matteo and L. Ackermann, *Chem. Sci.*, 2024, **15**, 19037–19043; (h) J. Pöhlmann, B. Yuan, J. Wu and L. Ackermann, *ACS Catal.*, 2025, **15**, 10542–10549; (i) S. Chen, Z. Xu, B. Yuan, X.-Y. Gou and L. Ackermann, *Nat. Synth.*, 2025, **4**, 655–663; (j) Y. Wang, B. Yuan, X. Chang and L. Ackermann, *Chem*, 2025, **11**, 102387; (k) A. Dey, R. Kancherla, K. Pal, N. Kloszewski and M. Rueping, *Commun. Chem.*, 2024, **7**, 295.
- 18 (a) T. Rogge, J. C. A. Oliveira, R. Kuniyil, L. Hu and L. Ackermann, *ACS Catal.*, 2020, **10**, 10551–10558; (b) L. Ackermann, *Chem. Rev.*, 2011, **111**, 1315–1345; (c) L. Ackermann, R. Vicente, H. K. Potukuchi and V. Pirovano, *Org. Lett.*, 2010, **12**, 5032–5035; (d) L. Ackermann, R. Vicente, H. K. Potukuchi and V. Pirovano, *Org. Lett.*, 2010, **12**, 5032–5035; (e) L. Ackermann, R. Vicente and A. Althammer, *Org. Lett.*, 2008, **10**, 2299–2302.

